Regulation of signal transduction pathways by hypoxia in breast cancer subtypes

Liu, Q.

Chapter 6

Exploring the role of CSE1L under hypoxia in breast cancer

Qiuyu Liu, Joannes T.M. Pruijs, Nasi Liu, Erik H.J. Danen, Sylvia E. Le Dévédec

Chapter 6

Abstract
Breast cancer is the most frequently diagnosed cancer in women. The high proliferative capacity of tumors can cause them to outgrow the reach of the vascular system, causing hypoxia. Here, we study CSE1L, a regulator of the Ran pathway, in breast cancer cells under normoxia and hypoxia. We find that increased CSE1L mRNA expression is observed preferentially in basal B cell lines and is associated in patients with decreased survival. In a targeted RNA-seq dataset, we noticed that exposure of basal-like breast cancer cells to chronic hypoxia downregulated CSE1L mRNA expression. Notably, CSE1L protein levels were similar and unaffected by hypoxia in luminal, basal A, and basal B cells but chronic hypoxia promoted CSE1L protein accumulation in the nucleus. Knockdown of CSE1L altered expression of EMT transcription factors, reduced expression of N-cadherin, and attenuated migration of basal A and B cell lines under chronic hypoxia. In a published dataset we identified a YAP/TAZ/TEAD binding site in the CSE1L gene. Silencing the WWTR1 gene encoding TAZ led to a further reduction of CSE1L mRNA expression under hypoxia and treatment with Verteporfin, an inhibitor of YAP/TAZ signaling, caused a reduction in CSE1L protein levels. Lastly, targeted RNAseq identified a CSE1L co-regulated network showing a shared downregulation in reponse to hypoxia and TAZ depletion that has clinical relevance in breast cancer. Together, these findings reveal new connections between hypoxia, TAZ, and CSE1L in breast cancer cells.

Keywords: breast cancer, hypoxia, CSE1L, EMT, migration, TAZ

Introduction

Cancer is the major cause of death around the world; incidence and mortality are anticipated to increase. In women, breast cancer is the most frequently diagnosed cancer and the common cause of cancer related death [1,2]. Breast cancer can be generally categorized depending on molecular markers. Classification depends on the presence of the progesterone receptor (PR), estrogen receptor (ER), and human epidermal growth factor Receptor 2 (HER2/neu) distinguishing 4 subtypes; luminal A (PR and/or ER positive, and HER2/neu negative), luminal B (PR and/or ER positive, HER2/neu positive), HER2-positive (PR and/or ER negative, and HER2/neu positive), and basal like/triple negative (PR and/or ER negative, and HER2/neu negative). Resistance to targeted treatment is associated with the basal like subtype which is also associated with poor prognosis [1].

The proliferative capacity of cancer cells causes the tumor to outgrow the reach of its surrounding vascular system resulting in decreased oxygen availability, called hypoxia [3]. The magnitude of the hypoxic state of cancer cells depends on the size and stage of the tumor [4]. Hypoxia-inducible factors (HIFs) are transcription factors regulating the primary response to hypoxic stress [5]. HIFs bind to hypoxia response elements (HREs) in the genome, regulating the hypoxic response associated with proliferation, invasion and angiogenesis [3,5]. Besides nuclear accumulation of HIFs, a commonly used hypoxia biomarker is carbonic anhydrase (CA)-9 upregulation, a target gene of HIF1α [6]. A distinction is made between acute and chronic hypoxia as cancer cells exhibit a different cellular response depending on the duration and frequency of hypoxia exposure [3,7,8]. Acute hypoxia is associated with reversible changes, chronic hypoxia is associated with long-term cellular adaptations potentially developing into mutagenesis and genetic instability [3]. Cellular responses to chronic hypoxia are incompletely understood. In an experimental setting, acute hypoxia is typically defined as exposure to 1% O_2 for up to 24 hours and chronic hypoxia as exposure to 1% O_2 for more than 1 day, up to several weeks [3,8].

CSE1L, also known as CAS (cellular apoptosis susceptibility) protein, is located on chromosomal region 20q13, which is amplified in various cancers and harbors several presumed oncogenes [9]. CSE1L is highly expressed in a variety of cancer types and corresponds with advanced cancer stage and poor patient outcome [10]. It functions as an export receptor for importin-alpha in the Ran-GTP nucleo-cytoplasmic transport pathway [10–12]. This function underlies its implication in many cellular functions including proliferation, invasion, apoptosis, and cancer metastasis [10,13]. CSE1L expression has been shown to be related to 'epithelial-to-mesenchymal transition' (EMT) in cancer and is involved in cell migration [14–16]. Classically, EMT is described to be a process where cells switch from an epithelial to mesenchymal phenotype [17]. It is known that EMT is not a binary process but rather a dynamic spectrum of intermediary phases expressing a cancer-type specific subset of EMT-markers [18,19]. 'Mesenchymal-to-epithelial transition' (MET), the reversed EMT process, develops as tumor cells arrive at distant organs to form secondary tumors [18]. Both processes play important roles in metastasis and clinical challenges arise as EMT/MET display opposite functions such as metastasis promoting or inhibiting activities in different contexts [18]. The epithelial-mesenchymal state of cells is regulated by a balance between pro-epithelial and pro-

mesenchymal transcription factors controlling expression of MMP-9 [20], Vimentin [21], β-catenin [22], N-cadherin [23], E-cadherin [23] and others. Additionally, the relationship between hypoxia and EMT has been extensively described [3,5,24,25]. A direct link between hypoxia, CSE1L and EMT has not been studied in breast cancer.

The Hippo signaling pathway is associated with hypoxia-induced tumor regulation. The main effectors of the Hippo pathway, 'yes-associated protein' (YAP) and 'transcriptional coactivator with PDZ-binding motif' (TAZ), have been identified to be downstream transcriptional targets for HIF1α [26,27]. As transcriptional coactivators, YAP and TAZ are known to regulate organ size, cell proliferation, and cell survival and their function is controlled by their cellular localization [28,29]. YAP/TAZ phosphorylation ensures their cytoplasmic localization so it can be degraded by the ubiquitin-proteasome pathway [26]. In the nucleus, YAP/TAZ are transcriptional coactivators associated with the TEAD-transcription factor family to promote expression of genes related to migration, tissue proliferation, and carcinogenesis [30]. A recent study reported that CSE1L promotes TAZ nuclear localization, TAZ mediated transcriptional activity, and malignancy in human lung cancer and glioblastoma cells [31]. Vice versa, transcriptomics analysis has recently identified CSE1L as a candidate target for YAP/TAZ/TEAD-mediated transcription [31].

Here, we explore the role of CSE1L under hypoxia in a panel of breast cancer cell lines representative of different subtypes. We discovered that hypoxia regulates CSE1L at transcriptional level and affects distribution of the CSE1L protein between nucleus and cytoplasm. We also show that under hypoxia CSE1L regulates aspects of EMT and cell migration in basal-like breast cancer cells. Our transcriptomics analysis supports earlier findings that CSE1L is a candidate YAP/TAZ/TEAD target and points to new connections between hypoxia, TAZ, and CSE1L in breast cancer cells.

Materials and methods

Cell culture

Nine human breast cancer cell lines were used overarching the luminal-, basal A-, and basal B-like breast cancer subtypes. These include the luminal-like MCF-7, T47D and BT474, basal A-like HCC1806, HCC1143 and SUM149PT, and basal B-like HCC38, MDA-MB-231 and Hs578t.

Cells were cultured in Gibco Roswell Park Memoria institute (RPMI) 1640 medium with 10% fetal bovine serum (FBS), 25 U/ml penicillin and 25 μg/ml streptomycin. Incubators were set for normoxia exposure (21% O_2) and hypoxia exposure (1% O_2).

Reagents

Verteporfin (Sigma-Aldrich, SML0534), CSE1L (GeneTex, GTX103005), CA9 (Novus, NB100-417), TAZ (Cell signal, E8E9), β-actin (Santa Cruz Biotechnology, sc-47778), Tubulin (Sigma-Aldrich, T-9026), N-cadherin (BD Biosciences, 610920), E-cadherin (BD Biosciences, 610181), Vimentin (Abcam, ab8069), HIF1α (BD Biosciences, 610959), HRP Anti-rabbit IgG (Jackson ImmunoResearch, 111-035-003), HRP Anti-mouse IgG (Jackson ImmunoResearch, 115-035-003). Hoechst 33258 (Thermo Fisher, 610959), Alexa 488 Anti-mouse IgG (Thermo Fisher, A-11001), Alexa 488 Anti-rabbit IgG (Thermo Fisher, A-11008).

RNA-Seq and TempO-Seq data analysis in cell lines

For TempO-Seq, cells were plated into 96-wells plates incubated at normoxia or hypoxia with WWTR1 knockdown (siLuciferase as control), after which the wells were washed once with ice cold PBS (Sigma, D8537-500ml), lysed using TempO-Seq lysis buffer (Bioclavis), and subsequently stored at -80 ˚C until shipment to BioClavis for TempO-Seq analysis [32]. Expression data were returned by BioClavis as counts per probe per treatment. An in-house R script was used for count normalization and determining differential gene expression. The library size (total number of reads per sample) was set as 100,000 reads and samples below this size were removed. DESeq2 package was used to normalize counts and calculate differentially expressed genes (DEGs). DEGs were filtered by $|\log_2 \text{Foldchange}| > 1$ and adjusted p-value (padj) < 0.05. Metascape, STRING protein, cBioPortal ('METABRIC, Nature 2012 & Nat Commun 2016' dataset), and Kaplan-Meier Plotter were used for analysis. A heatmap was made on the platform https://www.omicstudio.cn/tool (Lc-Bio Technologies Co., Lt.). RNA-seq data of 52 breast cancer cell lines [33] was used to identify differentially expressed genes (DEGs) in distinct breast cancer subtypes (basal A, basal B and luminal). RNA sequencing data from The Cancer Genome Atlas (TCGA) [34–36] was obtained using the January 2017 version of TCGA Assembler R package [37]. The log2 normalized values were used for further analyzing. Data from solid primary tumor tissue samples were used [38]. Gene expression in normal and tumor tissue was plotted in R v.3.6.3.

Immunohistochemical staining (IHC)

Immunohistochemical staining of CSE1L in normal tissue (patient ID: 2042), lobular carcinoma (patient ID: 614) and ductal carcinoma (patient ID: 659, 1271, 261) in breast cancer is available on The Human Protein Atlas (HPA). The detailed information is in Table S1.

Cell migration quantification assay

Cells were seeded in 20 µg/mL collagen coated 96-well plates at the proper density. After 5 days under hypoxia, cells were changed medium containing 1:10000 Hoechst (Thermo Fisher 33242) and incubated for 1 hour. Images were taken every 10 mins by Nikon Eclipse Ti microscope setting with with 21% O_2 or 1% O_2 using 20× objective. Analysis was using CellProfiler [39] and Rscript [40]. Plates were fixed later for SRB assay.

Sulforhodamine B (SRB) assay

96-well plates were used to seed cells for proper density to measure proliferation using the SRB assay. Cells were fixed adding 50% TCA (trichloroacetic acid) and plates were washed with demineralized water and air dried at room temperature (RT). 0.4% SRB was added per well. The plates were washed in 1% acetic acid and finally completely dried at RT. To extract the protein bound SRB, 10 mM Tris was added. A Fluostar OPTIMA plate reader was used to measure absorbance at 540nm.

siRNA mediated gene silencing

Gene silencing was performed by transfecting 50nM siGENOME human SMARTpool siRNA (GE Healthcare Dharmacon) into cells using INTERFERin (Westburg/PolyPlus) as transfection reagent. Medium change was performed after 15 hours. SiCSE1L and siWWTR1 were used for knockdown, Mock (H_2O) and siKinasePool were used as control.

Western blot

Cells were washed twice in ice cold 1× PBS (phosphate-buffered saline) and lysed using radioimmunoprecipitation (RIPA) buffer protease inhibitor cocktail (Sigma-Aldrich). The protein concentration was measured using bicinchoninic acid (BCA) assay. SDS-page gels were used for protein separation whereafter the proteins were transferred to a methanol-activated polyvinylidene difluoride (PVDF) membrane (Millipore, the Netherlands). Blocking the membranes was achieved using 5% BSA (bovine serum albumin, Sigma-Aldrich) solution. Primary antibody staining was performed overnight at 4°C. Chemiluminescence of HRP labeled secondary antibodies, stained using ECL (Thermo Fisher Scientific) or ECL-prime (Cytiva) before detecting, and Alexa labeled fluorescent was detected using an Amersham Imager 600 (GE Healthcare Life science).

Immunofluorescence

Cells were seeded at a density of 3000 cells/well in 96-well plates and cultured under hypoxia or normoxia for 5 days. Cells were washed with 1× DPBS (Dulbecco's phosphate-buffered saline) and fixed using 4% PFA (paraformaldehyde) and 0.3% Triton X-100. The cells were washed twice in 1× DPBS and blocking with 1% BSA. Primary antibody in 1% BSA is added to stain the cells overnight at 4°C. 3× washing using 1% BSA before adding secondary antibody in 1% BSA and incubate at room temperature (RT). Lastly, washing with 3× in DPBS before imaging with a Nikon Eclipse Ti microscope with a 20× objective and 50 µm scale bar in image. Quantification was done by Image J software (Intensity Ratio Nuclei Cytoplasm Tool, RRID: SCR_018573).

RNA-isolation and Real-Time quantitative PCR (RT-qPCR)

RNA-isolating was done using the RNeasy Kit (Qiagen). cDNA synthesis with the RevertAid H Minus First Strand cDNA Synthesis Kit (Thermo Fisher Scientific). RT-qPCR was performed in a 384-well PCR plate, containing 4 µL primer-mix and 6 µL cDNA-SYBRGreen PCR Mastermix (Applied Bioscience) solution, on a High-Resolution Melt Module for QuantStudioTM 6 Flex Real-Time PCR system. Gene expression was calculated using the 2^(-ΔΔCt) method after correction for β-actin. Primers used are: CSE1L (forward: 5' - ACACACAAAAATGACATCCCGT - 3', reverse: 5' - CCGCGTTCTAAGAATGCTTGA - 3'), Snail (forward: 5' - TGCTCCACAAGCACCAAGAGT - 3', reverse: 5' - TTCCATGGCAGTGAGAAGGAT - 3'), Slug (forward: 5' - GCCTCCAAAAAGCCAAACTACA - 3', reverse: 5' - AGGATCTCTGGTTGTGGTATGACA -3'), β-actin (forward: 5' - ATTGCCGACAGGATGCAGAA - 3', reverse: 5'- GCTGATCCACATCTGCTGGAA -3').

Statistical analysis

All statistical analysis was performed using GraphPad Prism 9. Statistical analysis was performed using t-test or one-way ANOVA. Data expresses mean ± SD. Significance is indicated by **** ($p < 0.0001$), *** ($p < 0.001$), ** ($p < 0.01$), * ($p < 0.05$), ns (not significant).

Results

CSE1L overexpression in breast cancer is associated with poor prognosis

CSE1L is highly expressed in a variety of cancer types and its high gene expression correlates with cancer stage and poor patient outcome [10]. We investigated its expression and clinical relevance in breast cancer. The chromosomal region 20q13

containing the CSE1L gene is often amplified, which is associated with the progression of various cancers [10,41]. Using our transcriptomics data of a panel of >50 human breast cancer cell lines [33], we found that CSE1L is highly expressed in all lines, in particular in the basal B subtype (Fig. 1A). Additionally, patient data from the TCGA database confirmed that expression of CSE1L was significantly higher in primary breast cancer tumors compared to healthy tissue (Fig. 1B). CSE1L expression is higher in ductal carcinoma rather than lobular carcinoma (Fig. 1C). We also used the "METABRIC, Nature 2012 & Nat Commun 2016" dataset, in which 1904 of 2173 samples showed copy number alterations (CNAs). As reported for other cancers, an increase in CSE1L expression was largely associated with an amplification of the CSE1L gene (Fig. 1D). Moreover, analysis using Kaplan-Meier plotter showed that expression of CSE1L in breast cancer was associated with a lower patient survival rate substantiating the clinical relevance of CSE1L in breast cancer (Fig. 1E).

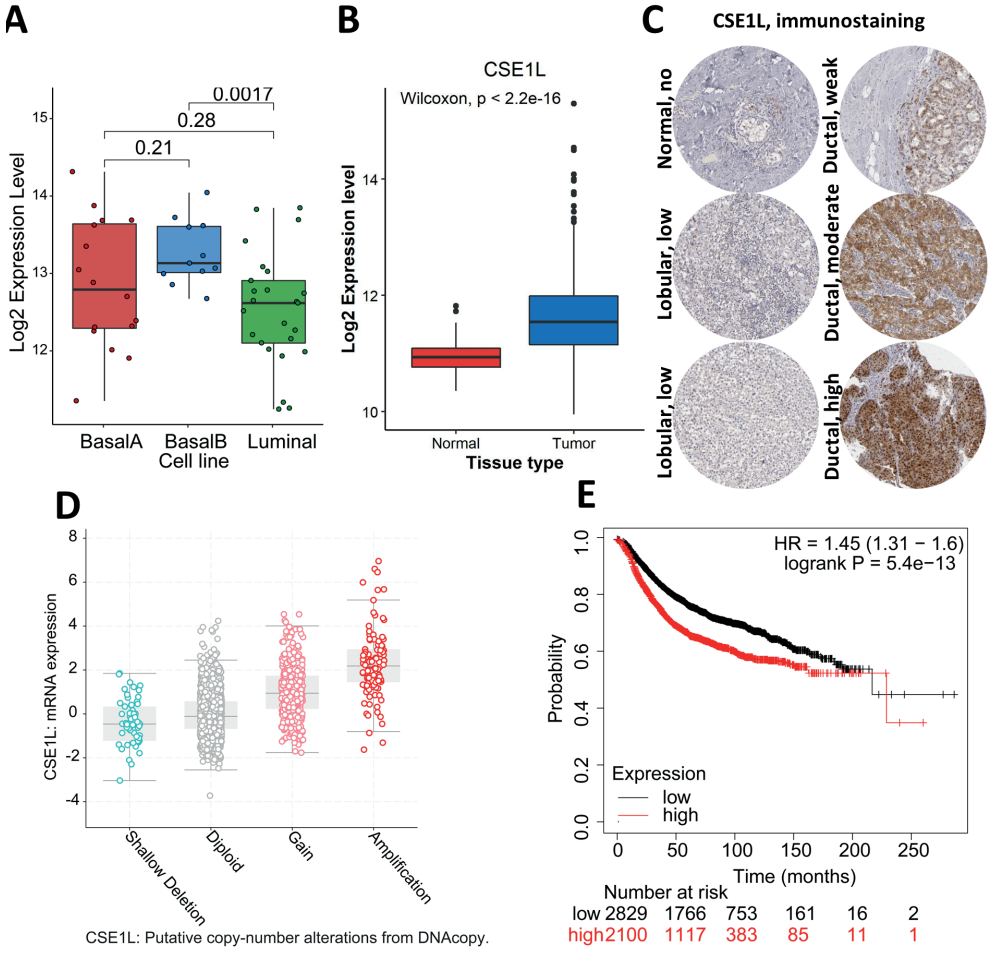

Figure 1. CSE1L expression in breast cancer. (A) Log_2RNA expression levels of CSE1L in >50 different cell lines classified as luminal-, basal A-, or basal B-like subtype (data obtained from RNA-seq dataset) [33]. p-value was calculated using One-way ANOVA. **(B)** Log_2RNA expression levels of CSE1L in tumor

and non-tumorous tissue in TGCA dataset. p-value calculated using Wilcoxon signed-rank test. **(C)** CSE1L protein levels in patient material (normal breast cancer, lobular carcinoma and ductal carcinoma tissues) detected using immunohistochemistry obtained from The Human Protein Atlas, Table S1. **(D)** CSE1L mutation copy number alterations by exploring the "METABRIC, Nature 2012 & Nat Commun 2016" dataset distinguishing shallow deletion, diploid, gain, and amplification. **(E)** Kaplan-Meier survival plot of CSE1L in 4929 breast cancer patients. Logrank <0.01 was considered significant for difference between high and low expressors.

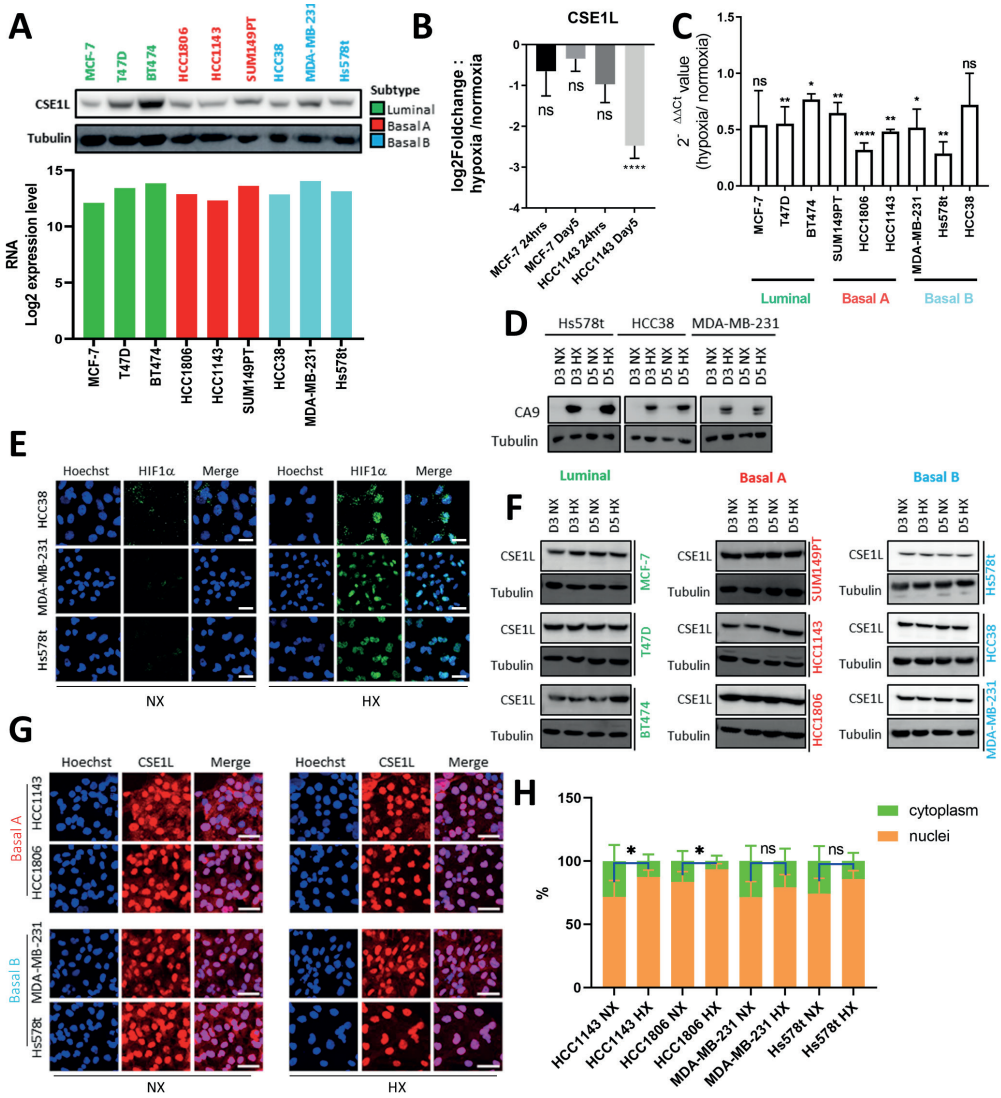

Figure 2. Effect of hypoxia on CSE1L expression in a selection of breast cancer cell lines. (A) CSE1L protein and RNA expression level in 9 breast cancer cell lines cultured in normoxia. Luminal-, basal A-, and basal B-like subtypes are indicated with green, red and blue respectively. **(B)** Log_2Foldchange expression of CSE1L in luminal-like MCF-7 and basal A-like HCC1143 breast cancer cells after 24 hours and 5 days hypoxia exposure compared to normoxia. **(C)** RT-qPCR analysis of CSE1L RNA expression in luminal-, basal A-, or basal B-like breast cancer cell lines after 5-day incubation in hypoxia compared to normoxia. 2^(-ΔΔCt) value (y-axis) is normalized with normoxia in each cell line. **(D)** CA9 protein

expression in basal B-like breast cancer cells exposed to 3- (D3) or 5-day (D5) normoxia (NX) or hypoxia (HX). **(E)** Immunofluorescence of HIF1α protein in cells were exposed to normoxia (NX) or hypoxia (HX) conditions for 3 days. **(F)** CSE1L protein expression in luminal-, basal A-, and basal B-like breast cancer cells detected with western blot. All cell lines were exposed to normoxia or hypoxia for 3 or 5 days. **(G)** Immunofluorescence of CSE1L protein in basal A, and basal B-like breast cancer cells after 5 days exposure to normoxia and hypoxia. **(H)** Quantification of CSE1L protein distribution between nucleus and cytoplasm using image analysis as described in M&M.

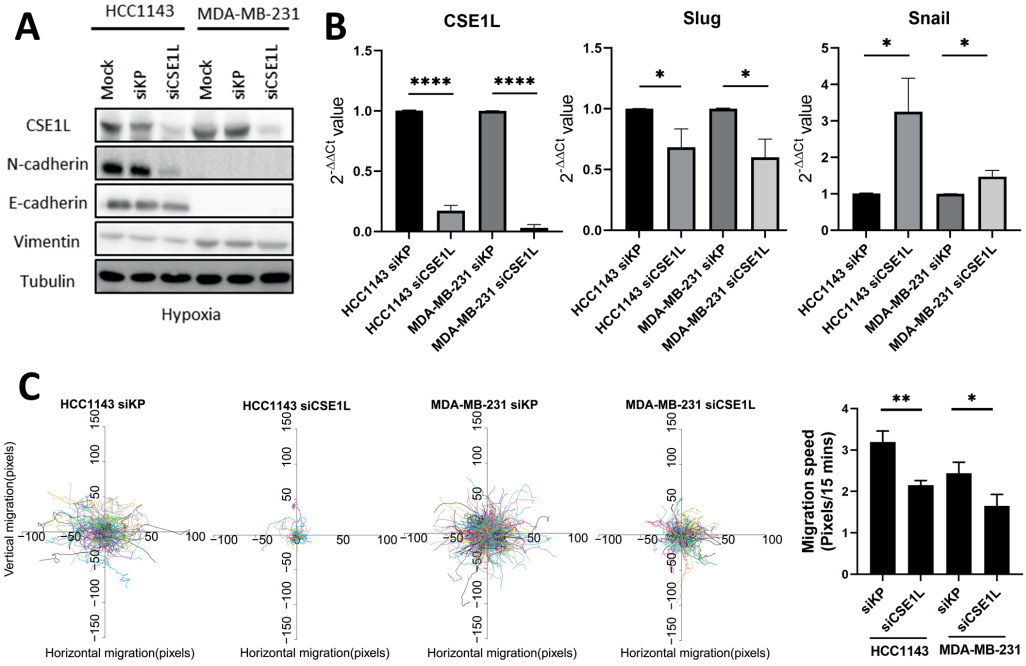

Figure 3. CSE1L regulates the migratory behavior of mesenchymal cells. (A) Western blot analysis for basal A-like (HCC1143) and basal B-like (MDA-MB-231) breast cancer cell lines after CSE1L knockdown (siCSE1L) with negative control of Mock and untreated control of siKinasePool (siKP) investigating EMT markers (N-cadherin, E-cadherin and Vimentin) under hypoxia for 5-day exposure. **(B)** CSE1L, Slug and Snail gene expression in HCC1143 and MDA-MB-231 breast cancer cells following CSE1L knockdown (siCSE1L) compared to siKinasePool (siKP) under hypoxia for 5-day exposure measured with RT-qPCR. **(C)** Selection of migratory tracks and quantification of migration speed of HCC1143 and MDA-MB-231 cells in hypoxia upon CSE1L knockdown (siCSE1L) normalized to siKinasePool (siKP).

CSE1L expression and subcellular localization in breast cancer cell lines under hypoxia

Recently published transcriptome data suggested differences in mRNA level between BC cell subtypes (Fig. 1A). We checked CSE1L levels in 3 luminal, 3 basal A, and 3 basal B breast cancer cell lines with both qPCR and western blot analysis and no subtype specific differences in CSE1L mRNA and protein level were observed in normoxia (Fig. 2A). Tumor hypoxia causes a rewiring of the transcriptional program which results in increased therapy resistance and aggressiveness [3]. Our previous findings demonstrated differential effects of acute (24 hours) and chronic (5 days) hypoxia in luminal and basal A cell lines (manuscript in submission). In a targeted RNA-seq (TempO-Seq) experiment, we observed that CSE1L showed a trend to be downregulated in

luminal MCF-7 and basal A HCC1143 cells after short exposure to hypoxia leading to a significant downregulation after 5-days hypoxia in the HCC1143 cells (Fig. 2B). We used qPCR to measure CSE1L mRNA levels in the same set of 9 cell lines exposed to chronic hypoxia. This showed that CSE1L mRNA was significantly decreased in almost all cell lines in response to hypoxia (Fig. 2C). To verify hypoxic conditions, we detected HIF1α localization and measured the expression of the HIF target, CA9. CA9 was clearly upregulated and HIF1α accumulated in the nuclei of 3 basal B cell lines after exposure to 3 days of hypoxia (Fig. 2D & E). Next, we analyzed CSE1L protein expression after 3- and 5-days hypoxia exposure in the set of cell lines using western blot analysis. In contrast to mRNA analysis, CSE1L protein expression was unchanged even though RNA expression was decreased in most of the cell lines between normoxia and hypoxia (Fig. 2C & F). As CSE1L is known to function as a nucleo-cytoplasmic exporter, we wondered if the localization of the protein might be then altered upon hypoxia exposure [42,43]. Immunofluorescence and image quantification showed a slight but significant increase in nuclear accumulation of CSE1L in HCC1143 and HCC1806 cells under hypoxia (Fig. 2G & H). A similar but not significant trend was observed in MDA-MB-231 and Hs578t cells. Taken together, hypoxia induces a reduction of CSE1L mRNA, which does not lead to a change in CSE1L protein expression but CSE1L subcellular localization is shifted more towards the nucleus in basal A breast cancer cell lines.

CSE1L regulates aspects of EMT and contributes to cell migration in basal-like breast cancer cells

Since CSE1L is associated with several EMT markers in different cancer types and its subcellular localization appeared affected under hypoxia, we would like to know if it plays a role in the mesenchymal phenotype of basal A and B cells [14,16]. To realize this, we selected HCC1143 (basal A/pre-EMT) and MDA-MB-231 (basal B/post-EMT) cells to evaluate the effect of siRNA mediated knockdown of CSE1L (Fig. 3A & B). N-cadherin levels decreased in HCC1143 cells depleted of CSE1L, but no changes in the levels of E-cadherin and Vimentin level were observed (Fig. 3A). Next, we evaluated the effect on mRNA levels of Slug and Snail, two transcription factors involved in EMT [44,45]. While Slug transcripts were lower upon CSE1L depletion, Snail transcripts were increased in both basal-like breast cancer cell lines (Fig. 3B). Finally, we checked how cell motility was affected upon CSE1L knockdown under hypoxic conditions. The results of an image-based random cell migration assay showed that cell migration speed was reduced after CSE1L knockdown under hypoxia (Fig. 3C) and less cell proliferation was also measured (Fig. S1B). Overall, knockdown of CSE1L affects some of the EMT markers and regulators and impairs the migratory capacity of mesenchymal cells.

Cross talk between hypoxia and TAZ in regulating CSE1L expression

We explored published transcriptomics data [46] and identified CSE1L as a candidate target gene of YAP/TAZ/TEAD. We next used high throughput targeted sequencing to analyze the impact of TAZ depletion on the expression of CSE1L in HCC1143 cells under normoxia and hypoxia. WWTR1 (the gene name of TAZ) mRNA was not significantly affected by the oxygen level and it was efficiently decreased by siWWTR1 under normoxia and hypoxia (Fig. 4A). However, the CSE1L mRNA level was significantly decreased under hypoxia (HX/NX) and even further decreased by siWWTR1 (versus control luciferase siRNA) under hypoxia ([siWWTR1/siLuc] HX) while siWWTR1 did not

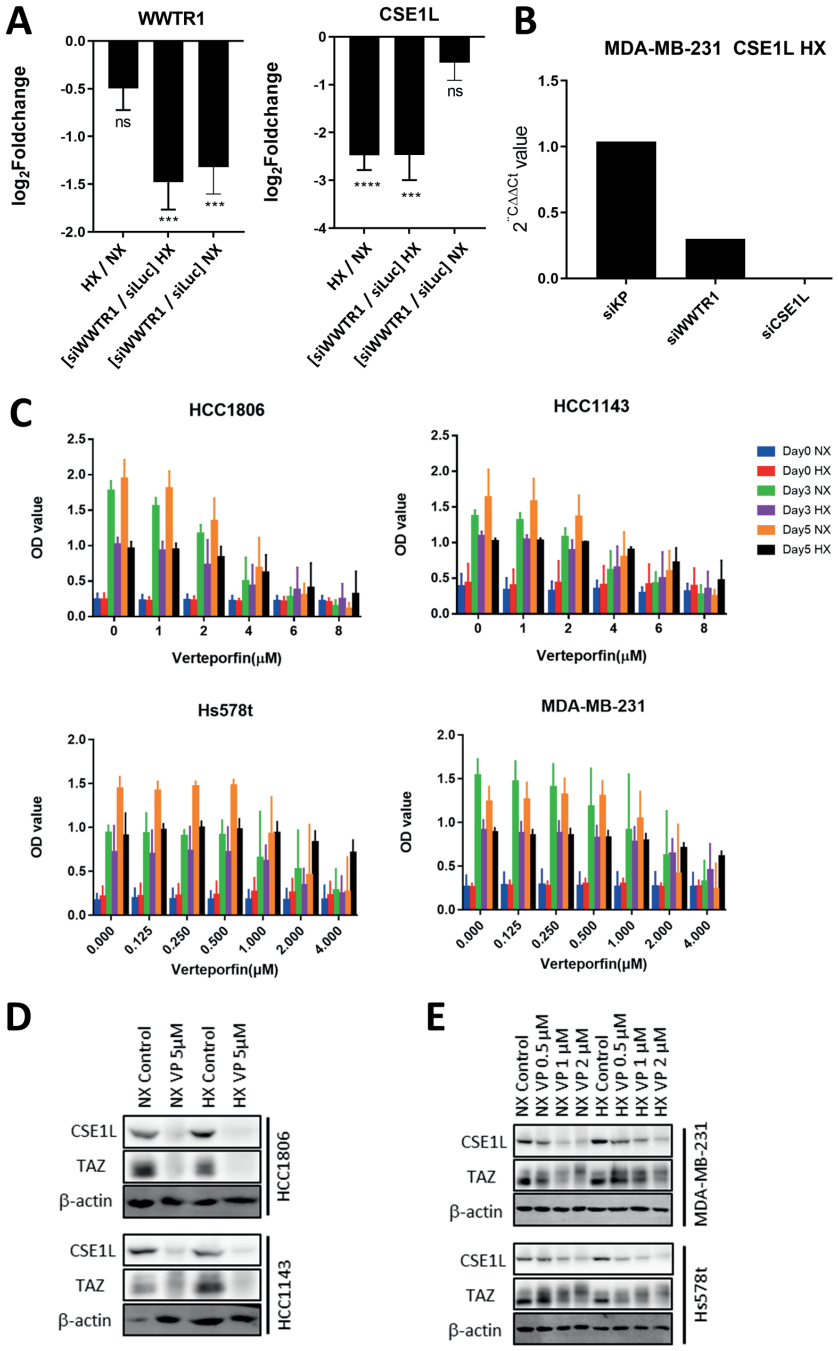

Figure 4. Crosstalk between TAZ and hypoxia on CSE1L expression. (A) Log_2Foldchange expression of WWTR1 and CSE1L in HCC1143 cells cultured in 5 days hypoxia HX/NX, [siWWTR1/ siLuc] HX and [siWWTR1/ siLuc] NX. 1) HCC1143 cells were cultured with medium under normoxia (NX, control) and hypoxia (HX) for 5 days. HX/ NX means that the data was normalized to NX; 2) RNA mediated

TAZ knockdown (siWWTR1) was conducted in HCC1143 cells and knockdown of Luciferase was used as control (siLuciferase) under hypoxia (HX) and normoxia (NX) for 5 days. [siWWTR1/ siLuc] means that the data was normalized to siLuciferase. **(B)** RNA expression of CSE1L upon WWTR1 and CSE1L knockdown under hypoxia in MDA-MB-231 cell line, with siKinasePool as control (n=1 only). **(C)** Quantification of proliferation of basal A-like (HCC1806 and HCC1143) and basal B-like (Hs578t and MDA-MB-231) breast cancer cell lines using the SRB assay following 0, 3 or 5-day normoxia or hypoxia exposure upon addition of 0-8 µM (basal A) or 0-4 µM (basal B) of Verteporfin. OD value indicates the absorption of sulforhodamine B. **(D, E)** Western blot analysis for basal A-like (D) and basal B-like (E) breast cancer cells for CSE1L and TAZ protein expression following 3-day normoxia or hypoxia exposure in addition to 5 µM Verteporfin (D), 0.5-2 µM Verteporfin (E), using 0.1% DMSO as control vehicle.

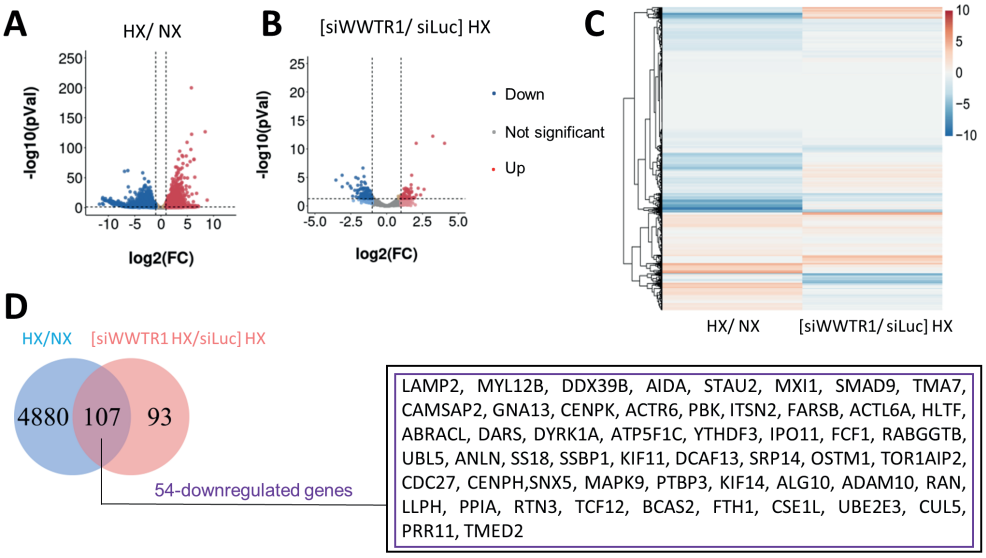

Figure 5. Overview of whole transcriptome analysis of HCC1143 cells cultured for 5 days in hypoxia with/without depletion of WWTR1. Volcano plot of differentially expressed genes HX/NX **(A)** and [siWWTR1/ siLuc] HX **(B)** with down-regulated (blue), up-regulated (red) and not significant genes (grey). **(C)** Unsupervised clustering of all genes (log_2Foldchange) in HX/ NX and [siWWTR1/ siLuc] HX conditions. **(D)** Venn diagram of HX/ NX (blue) and [siWWTR1/ siLuc] HX (pink); the box lists the 54 of the 107 overlapping DEGs that were downregulated both in HX/ NX and in [siWWTR1/ siLuc] HX. DEGs were filtered by |log_2Foldchange| >1 and padj <0.05.

affect CSE1L mRNA levels under normoxia (Fig. 4A). qPCR analysis of MDA-MB-231 cells confirmed the downregulation of CSE1L in the presence of siWWTR1 under hypoxia (Fig. 4B). We next tested the impact of Verteporfin, a known inhibitor of YAP/TAZ-TEAD transcriptional activity [47,48] on CSE1L expression. We first determined the cytotoxicity of this compound on basal A and basal B breast cancer cell lines with the SRB assay (Fig. 4C). Interestingly, the IC50 was higher for basal A cells (HCC1806 and HCC1143; 5 µM) than for basal B cells (Hs578t and MDA-MB-231; 2 µM). Exposure of the same cell lines to Verteporfin concentrations up to the IC50 caused a concentration dependent decrease of TAZ as expected, which was accompanied by a decrease of CSE1L (Fig. 4D-E & S1A). These results suggest that CSE1L protein expression can be inhibited by YAP/ TAZ/TEAD inhibition.

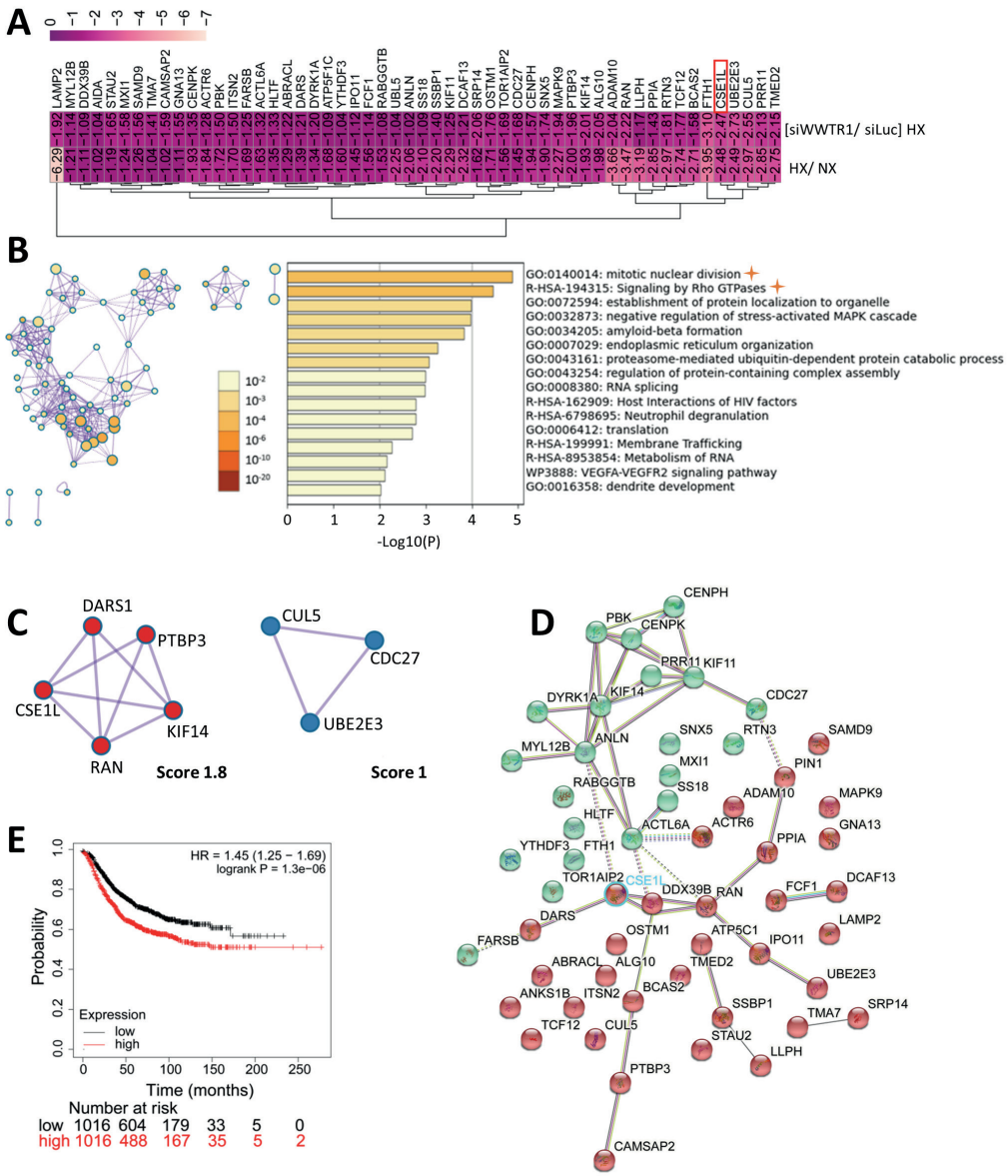

Figure 6. Enrichment analysis and clinical relevance of the 54 down-regulated DEGs. (A) Heatmap of the 54 down-regulated DEGs both in HX/ NX and [siWWTR1/ siLuc] HX. Log_2Foldchange expression value is showed. **(B)** Enrichment analysis of the 54 down-regulated DEGs using the Metascape platform. One GO term is per cluster, which is colored according to p-value. The terms related to CSE1L are labelled with a yellow star. **(C)** Molecular complex detection (MCODE) network shows two clusters derived from the 54 down-regulated DEGs. Score of the red one is 1.8 and the blue one is 1. **(D)** STRING protein network of 54 down-regulated DEGs is divided over 2 clusters (red and green) and separated by dotted lines. CSE1L is indicated in light blue at the edge between the two clusters. **(E)** Kaplan-Meier (KM) curve for the mean expression of the 54 down-regulated DEGs in breast cancer patients. Logrank <0.01 was considered significant for difference between high and low expressors.

A CSE1L containing gene network with clinical relevance regulated by hypoxia and TAZ
We further analyzed the transcriptomics data of HX/NX and [siWWTR1/siLuc] HX. The reponse to hypoxia gave rise to more differentially expressed genes than the reponse to siWWTR1 under hypoxia and both showed a similarly equal distribution of up- and down-regulated genes (Fig. 5A & B). Interestingly, all genes that were differentially expressed in hypoxia showed a change in the same direction in reponse to siWWTR1 under hypoxia but some opposite regulation was also observed (Fig. 5C). Almost 5000 differentially expressed genes were identified in HCC1143 cells exposed to long-term hypoxia when compared to normoxia ($|\log_2 FC| > 1$ and p-adjusted value <0.05) (Fig. 5D). Only 200 genes were differentially expressed in HCC1143 cells treated with siWWTR1 versus siLuc under hypoxia. Of those 200 genes, 107 genes overlapped between HX/NX and [siWWTR1/siLuc] HX. 54 genes followed the same patern as CSE1L: they were down-regulated under hypoxia and even further downregulated in response to TAZ depletion under that same condition (Fig. 6A). Of the clusters generated from these 54 genes by Metascape, the two most significantly enriched pathways were related to mitotic nuclear division and Rho GTPase signaling and both harbored CSE1L (Fig. 6B). Next, we applied the Molecular Complex Detection (MCODE) algorithm to the network of the top 16 clusters to identify modules in which proteins are densely interacting. Two modules were identified with score 1.8 (KIF14, CSE1L, PTBP3, RAN, DARS1) and score 1 (CDC27, CUL5, UBE2E3) respectively (Fig. 6C). STRING analysis gave a PPI enrichment p-value of 6.27e-05 indicating significantly enriched interactions between the proteins encoded by the 54 down-regulated genes, and it showed a division over two sub-clusters (Fig. 6D) where CSE1L is interestingly at the edge. Lastly, clinical impact of the 54 down-regulated genes was analyzed using the KM plotter platform. A higher mean expression of the 54 genes was associated with a lower probability of relapse-free survival in a cohort of breast cancer patients (HR, 1.45; p, 1.3e-06) (Fig. 6E). Of note, no significant association was detected when a cohort of TNBC patients was selected (not shown). Taken together, our data show that hypoxia and TAZ regulate CSE1L mRNA levels and a CSE1L co-regulated network that has clinical relevance in breast cancer.

Discussion
CSE1L is associated with a multitude of cellular processes including proliferation, apoptosis and metastasis and its chromosomal region, 20q13, is known to be overexpressed in several cancers, including colorectal cancer, ovarian cancer and breast cancer, which correlates with poor patient outcome [9,10,13,49,50]. Our study extends these findings showing that CSE1L mRNA expression is particularly increased in basal B cells in a broad panel of >50 human breast cancer cell lines. Moreover, we show that the highest CSE1L mRNA expression levels are associated with amplifications and, in line with earlier work, CSE1L expression is inversely correlated with patient survival.

In agreement with previously described roles for CSE1L in EMT and cell migration [16,51–54], we find that siRNA mediated CSE1L knockdown under hypoxia reduces migratory potential of basal-like breast cancer cells and leads to reduced N-cadherin protein expression in basal A HCC1143 cells. However, we do not observe effects on Vimentin and E-cadherin and two transcription factors known to promote EMT, Snail and Slug [55,56], are affected in opposite directions. It therefore remains to be determined whether EMT or other mechanisms explain the association of CSE1L with cell migration.

As CSE1L levels as well as hypoxia are associated with poor survival, it appears surprising that we observe that CSE1L mRNA is downregulated in response to hypoxia. CSE1L has not been previously studied in the context of hypoxia. Notably, altered CSE1L mRNA levels under hypoxia are not translated to changes at the protein level and may therefore have no functional consequence. However, given its role as an export receptor for importin-alpha in the Ran-GTP nucleo-cytoplasmic transport pathway [10–12], our finding that CSE1L localization shifts towards more nuclear localization may be important as the Ran pathway plays a critical role in cell function from polarity to cell division [57]. Indeed, in addition to attenuated migration we observe a growth inhibition in breast cancer cells depleted of CSE1L in hypoxia.

With the analysis of published transcriptomics data, we find that CSE1L is a candidate YAP/TAZ/TEAD target gene and CSE1L has been implicated in regulation of TAZ translocation [31,46]. Our own work has indicated that TAZ, but not YAP, is subject to regulation by hypoxia in basal breast cancer cells [58]. Given the potential cross talk between hypoxia, TAZ, and CSE1L, we explored the effect of TAZ depletion on CSE1L expression under normoxia and hypoxia. The finding that CSE1L mRNA levels are reduced under hypoxia and then further reduced by siWWTR1, whereas siWWTR1 has no effect on CSE1L mRNA under normoxia indeed suggests that hypoxia and TAZ cooperate in transcriptional regulation of CSE1L. The biological relevance of this observation is unclear since, as mentioned above, changes in CSE1L mRNA did not coincide with changes in protein level.

Our finding that inhibition of YAP/TAZ-TEAD using Verteporfin did attenuate CSE1L protein levels may be unrelated to the effects observed at the transcriptional level. Moreover, apart from the effect of Verteporfin on YAP/TAZ-TEAD interaction, it has been shown that the inhibitor also alters the Ras-ERK signalling route [59]. Notably, in that work ERK, p-ERK, and p-AKT levels were decreased in human leukaemia NB4 cells exposed to 10 and 20 μM Verteporfin for 24hrs. In our hands, this was far above the IC50 value and expected to lead to severe cytotoxicity. Nevertheless, as Ras-ERK activity has been reported to regulate CSE1L phosphorylation and trafficking in different cancer types [13,61,62] and Akt activity has been reported to drive CSE1L nuclear localization [50], these activities may underlie the effect of Verteporfin on CSE1L protein expression. Further research is required to explore the relative roles of YAP/TAZ/TEAD versus ERK and AKT in the mechanism of action of Verteporfin towards CSE1L.

The pathway analysis of the genes downregulated in response to hypoxia and TAZ knockdown revealed two co-regulated networks of which one is related to cell cycle (green cluster, Fig. 6D) and the other one to nuclear-cytoplasmic shuttling (red cluster, Fig. 6D) with CSE1L being at the interface between the two clusters. The identification of the cell cycle-related gene network supports earlier reports which described CSE1L as a proliferation-associated protein in different types of cancer including breast cancer [10,60,61]. CSE1L depletion affected the proliferation of several cell lines in hypoxic conditions. Additionally, CSE1L is known as a nucleocytoplasmic shuttling protein regulating protein transport which does explain the identification of the nuclear-cytoplasmic related gene network [11,62]. In particular, the RAN pathway which includes CSE1L has been implicated in TAZ nuclear shuttling by interacting with importin α5 [31].

Additionally, HIF1α has been also shown to mediate TAZ expression and translocation [63] suggesting a potential interaction between all three nuclear proteins: HIF1α, CSE1L and TAZ. Further scrutinization of a potential role of CSE1L in the nuclear-cytoplasimc shuttling of TAZ and HIF1α during hypoxia is needed. Overall, our findings reveal new connections between hypoxia, TAZ, and CSE1L in breast cancer cells and confirm the clinical relevance of CSE1L in breast cancer [10,11,13,60,64].

Author Contributions

Qiuyu Liu: Investigation, Validation, Writing - Original Draft; Joannes T.M. Pruijs: Validation, Writing - Original Draft; Nasi Liu: Validation; Sylvia E. Le Dévédec and Erik H.J. Danen: Writing - Original Draft, Writing - review & editing, Supervision

Acknowledgments

Qiuyu Liu and Nasi Liu were financially supported by the China Scholarship Council.

References

1.Fahad Ullah, M. Breast Cancer: Current Perspectives on the Disease Status. Advances in experimental medicine and biology 1152, 51–64 (2019).
2.Sung, H. et al. Global Cancer Statistics 2020: GLOBOCAN Estimates of Incidence and Mortality Worldwide for 36 Cancers in 185 Countries. CA: a cancer journal for clinicians 71, 209–249 (2021).
3.Muz, B., La Puente, P. de, Azab, F. & Azab, A. K. The role of hypoxia in cancer progression, angiogenesis, metastasis, and resistance to therapy. Hypoxia (Auckland, N.Z.) 3, 83–92 (2015).
4.Walsh, J. C. et al. The clinical importance of assessing tumor hypoxia: relationship of tumor hypoxia to prognosis and therapeutic opportunities. Antioxidants & redox signaling 21, 1516–1554 (2014).
5.Majmundar, A. J., Wong, W. J. & Simon, M. C. Hypoxia-inducible factors and the response to hypoxic stress. Molecular cell 40, 294–309 (2010).
6.Span, P. N., Bussink, J., Manders, P., Beex, L. V. A. M. & Sweep, C. G. J. Carbonic anhydrase-9 expression levels and prognosis in human breast cancer: association with treatment outcome. British journal of cancer 89, 271–276 (2003).
7.Bayer, C. & Vaupel, P. Acute versus chronic hypoxia in tumors: Controversial data concerning time frames and biological consequences. Strahlentherapie und Onkologie : Organ der Deutschen Rontgengesellschaft ... [et al] 188, 616–627 (2012).
8.Liu, Q., Palmgren, V. A. C., Danen, E. H. & Le Dévédec, S. E. Acute vs. chronic vs. intermittent hypoxia in breast Cancer: a review on its application in in vitro research. Molecular biology reports; 10.1007/s11033-022-07802-6 (2022).
9.Aust, D. E. et al. Prognostic relevance of 20q13 gains in sporadic colorectal cancers: a FISH analysis. Scandinavian journal of gastroenterology 39, 766–772 (2004).
10.Jiang, M.-C. CAS (CSE1L) signaling pathway in tumor progression and its potential as a biomarker and target for targeted therapy. Tumour biology : the journal of the International Society for Oncodevelopmental Biology and Medicine 37, 13077–13090 (2016).
11.Behrens, P., Brinkmann, U. & Wellmann, A. CSE1L/CAS: its role in proliferation and apoptosis. Apoptosis : an international journal on programmed cell death 8, 39–44 (2003).
12.Kau, T. R., Way, J. C. & Silver, P. A. Nuclear transport and cancer: from mechanism to intervention. Nature reviews. Cancer 4, 106–117 (2004).
13.Ye, M. et al. Cellular apoptosis susceptibility protein (CAS) suppresses the proliferation of breast cancer cells by upregulated cyp24a1. Medical oncology (Northwood, London, England) 37, 43 (2020).
14.Liao, C.-F. et al. CSE1L, a novel microvesicle membrane protein, mediates Ras-triggered microvesicle generation and metastasis of tumor cells. Molecular medicine (Cambridge, Mass.) 18, 1269–1280 (2012).
15.Tanabe, S. et al. Molecular Network Profiling in Intestinal- and Diffuse-Type Gastric Cancer. Cancers 12 (2020).
16.Wang, Y.-S., Peng, C., Guo, Y. & Li, Y. CSE1L promotes proliferation and migration in oral cancer through positively regulating MITF. European review for medical and pharmacological sciences 24, 5429–5435 (2020).
17.Sun, D., Baur, S. & Hay, E. D. Epithelial-mesenchymal transformation is the mechanism for fusion of the craniofacial primordia involved in morphogenesis of the chicken lip. Developmental biology 228, 337–349 (2000).
18.Nieto, M. A., Huang, R. Y.-J., Jackson, R. A. & Thiery, J. P. EMT: 2016. Cell 166, 21–45 (2016).
19.Cook, D. P. & Vanderhyden, B. C. Context specificity of the EMT transcriptional response. Nature communications 11, 2142 (2020).
20.Li, Y. et al. Role of MMP-9 in epithelial-mesenchymal transition of thyroid cancer. World journal of surgical oncology 18, 181 (2020).
21.Liu, C.-Y., Lin, H.-H., Tang, M.-J. & Wang, Y.-K. Vimentin contributes to epithelial-mesenchymal transition cancer cell mechanics by mediating cytoskeletal organization and focal adhesion maturation. Oncotarget 6, 15966–15983 (2015).
22.Mahmood, M. Q. et al. β-catenin, Twist and Snail: Transcriptional regulation of EMT in smokers and COPD, and relation to airflow obstruction. Scientific reports 7, 10832 (2017).
23.Loh, C.-Y. et al. The E-Cadherin and N-Cadherin Switch in Epithelial-to-Mesenchymal Transition: Signaling, Therapeutic Implications, and Challenges. Cells 8 (2019).
24.Tam, S. Y., Wu, V. W. C. & Law, H. K. W. Hypoxia-Induced Epithelial-Mesenchymal Transition in Cancers: HIF-1α and Beyond. Frontiers in oncology 10, 486 (2020).
25.Northey, J. J., Przybyla, L. & Weaver, V. M. Tissue Force Programs Cell Fate and Tumor Aggression. Cancer discovery 7, 1224–1237 (2017).
26.Zhao, C. et al. Yes-associated protein (YAP) and transcriptional coactivator with a PDZ-binding motif (TAZ): a nexus between hypoxia and cancer. Acta pharmaceutica Sinica. B 10, 947–960 (2020).
27.Zanconato, F., Cordenonsi, M. & Piccolo, S. YAP/TAZ at the Roots of Cancer. Cancer cell 29, 783–803 (2016).
28.Pocaterra, A., Romani, P. & Dupont, S. YAP/TAZ functions and their regulation at a glance. Journal of cell science 133 (2020).
29.Zanconato, F., Cordenonsi, M. & Piccolo, S. YAP and TAZ: a signalling hub of the tumour microenvironment.

Nature reviews. Cancer 19, 454–464 (2019).
30.Zhang, K. et al. YAP and TAZ Take Center Stage in Cancer. Biochemistry 54, 6555–6566 (2015).
31.Nagashima, S. et al. CSE1L promotes nuclear accumulation of transcriptional coactivator TAZ and enhances invasiveness of human cancer cells. The Journal of biological chemistry 297, 100803 (2021).
32.Yeakley, J. M. et al. A trichostatin A expression signature identified by TempO-Seq targeted whole transcriptome profiling. PloS one 12, e0178302 (2017).
33.Koedoot, E. et al. Differential reprogramming of breast cancer subtypes in 3D cultures and implications for sensitivity to targeted therapy. Scientific reports 11, 7259 (2021).
34.Comprehensive molecular portraits of human breast tumours. Nature 490, 61–70 (2012).
35.Ciriello, G. et al. Comprehensive Molecular Portraits of Invasive Lobular Breast Cancer. Cell 163, 506–519 (2015).
36.Tavernier, J. et al. Expression of human and murine interleukin-5 in eukaryotic systems. DNA (Mary Ann Liebert, Inc.) 8, 491–501 (1989).
37.Zhu, Y., Qiu, P. & Ji, Y. TCGA-assembler: open-source software for retrieving and processing TCGA data. Nature methods 11, 599–600 (2014).
38.Koedoot, E. et al. Co-regulated gene expression of splicing factors as drivers of cancer progression. Scientific reports 9, 5484 (2019).
39.Carpenter, A. E. et al. CellProfiler: image analysis software for identifying and quantifying cell phenotypes. Genome biology 7, R100 (2006).
40.Wink, S. et al. Quantitative high content imaging of cellular adaptive stress response pathways in toxicity for chemical safety assessment. Chemical research in toxicology 27, 338–355 (2014).
41.Gao, S.-P. et al. High expression of COX5B is associated with poor prognosis in breast cancer. Future oncology (London, England) 13, 1711–1719 (2017).
42.Çağatay, T. & Chook, Y. M. Karyopherins in cancer. Current opinion in cell biology 52, 30–42 (2018).
43.Kutay, U., Bischoff, F.R., Kostka, S., Kraft, R. & Görlich, D. Export of Importin α from the Nucleus Is Mediated by a Specific Nuclear Transport Factor. Cell 90, 1061–1071 (1997).
44.Martin, T. A., Goyal, A., Watkins, G. & Jiang, W. G. Expression of the transcription factors snail, slug, and twist and their clinical significance in human breast cancer. Annals of surgical oncology 12, 488–496 (2005).
45.Kang, E., Seo, J., Yoon, H. & Cho, S. The Post-Translational Regulation of Epithelial-Mesenchymal Transition-Inducing Transcription Factors in Cancer Metastasis. International journal of molecular sciences 22 (2021).
46.Zanconato, F. et al. Genome-wide association between YAP/TAZ/TEAD and AP-1 at enhancers drives oncogenic growth. Nature cell biology 17, 1218–1227 (2015).
47.Gibault, F. et al. Molecular Features of the YAP Inhibitor Verteporfin: Synthesis of Hexasubstituted Dipyrrins as Potential Inhibitors of YAP/TAZ, the Downstream Effectors of the Hippo Pathway. ChemMedChem 12, 954–961 (2017).
48.Giraud, J. et al. Verteporfin targeting YAP1/TAZ-TEAD transcriptional activity inhibits the tumorigenic properties of gastric cancer stem cells. International journal of cancer 146, 2255–2267 (2020).
49.Pimiento, J. M. et al. Knockdown of CSE1L Gene in Colorectal Cancer Reduces Tumorigenesis in Vitro. The American journal of pathology 186, 2761–2768 (2016).
50.Salvi, A. et al. PHY34 inhibits autophagy through V-ATPase V0A2 subunit inhibition and CAS/CSE1L nuclear cargo trafficking in high grade serous ovarian cancer. Cell death & disease 13, 45 (2022).
51.Alnabulsi, A. et al. Cellular apoptosis susceptibility (chromosome segregation 1-like, CSE1L) gene is a key regulator of apoptosis, migration and invasion in colorectal cancer. The Journal of pathology 228, 471–481 (2012).
52.Tai, C.-J. et al. Increased cellular apoptosis susceptibility (CSE1L/CAS) protein expression promotes protrusion extension and enhances migration of MCF-7 breast cancer cells. Experimental cell research 316, 2969–2981 (2010).
53.Liu, C. et al. CSE1L participates in regulating cell mitosis in human seminoma. Cell proliferation 52, e12549 (2019).
54.Li, Y. et al. CSE1L silence inhibits the growth and metastasis in gastric cancer by repressing GPNMB via positively regulating transcription factor MITF. Journal of cellular physiology 235, 2071–2079 (2020).
55.Wang, Y., Shi, J., Chai, K., Ying, X. & Zhou, B. P. The Role of Snail in EMT and Tumorigenesis. Current cancer drug targets 13, 963–972 (2013).
56.Sterneck, E., Poria, D. K. & Balamurugan, K. Slug and E-Cadherin: Stealth Accomplices? Frontiers in molecular biosciences 7, 138 (2020).
57.Ozugergin, I. & Piekny, A. Complementary functions for the Ran gradient during division. Small GTPases 12, 177–187 (2021).
58.Liu, Q. et al. Hypoxia Triggers TAZ Phosphorylation in Basal A Triple Negative Breast Cancer Cells. International journal of molecular sciences 23 (2022).
59.Chen, M. et al. Verteporfin Inhibits Cell Proliferation and Induces Apoptosis in Human Leukemia NB4 Cells without Light Activation. International journal of medical sciences 14, 1031–1039 (2017).
60.Behrens, P., Brinkmann, U., Fogt, F., Wernert, N. & Wellmann, A. Implication of the proliferation and apoptosis associated CSE1L/CAS gene for breast cancer development. Anticancer research 21, 2413–2417 (2001).
61.Zhang, X. et al. CSE1L, as a novel prognostic marker, promotes pancreatic cancer proliferation by regulating the AKT/mTOR signaling pathway. Journal of Cancer 12, 2797–2806 (2021).
62.Cook, A. et al. The structure of the nuclear export receptor Cse1 in its cytosolic state reveals a closed conformation incompatible with cargo binding. Molecular cell 18, 355–367 (2005).
63.Xiang, L. et al. Hypoxia-inducible factor 1 mediates TAZ expression and nuclear localization to induce the breast cancer stem cell phenotype. Oncotarget 5, 12509–12527 (2014).
64.Ye, M. et al. Interfering with CSE1L/CAS inhibits tumour growth via C3 in triple-negative breast cancer. Cell proliferation 55, e13226 (2022).

Supplemental data

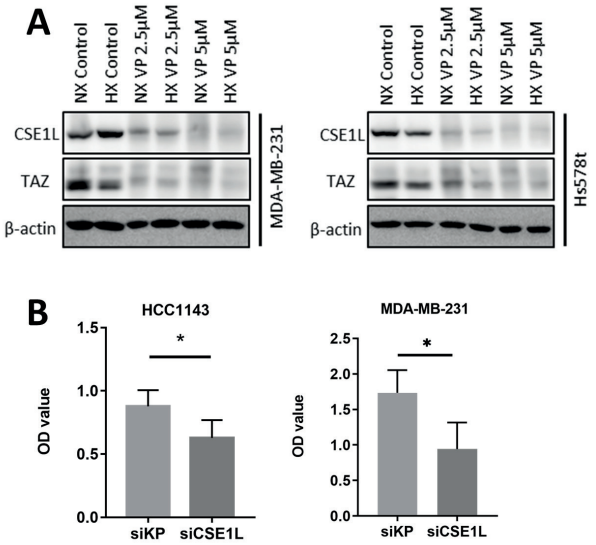

Figure S1. (A) Western blot analysis for CSE1L and TAZ protein expression following 72-hours normoxia or hypoxia exposure in addition to 2.5 or 5 µM Verteporfin, and 0.1% DMSO (control). **(B)** Quantification of cell proliferation of the basal A-like (HCC1143) and basal B-like (MDA-MB-231) cell lines upon CSE1L gene knockdown (siCSE1L) compared to siKinasePool (siKP).

Table S1. Metadata of immunohistochemical staining of CSE1L in breast tumor samples from Human Protein Atlas

Sample ID	Type cancer	tumor cells	Weblink in Human Protein Atlas
Female, age 75 Breast (T-04000) Normal tissue, NOS (M-00100) Patient id: 2042	normal tissue	negative	https://www.proteinatlas.org/ENSG00000124207-CSE1L/tissue/breast#img
Female, age 85 Breast (T-04000) Lobular carcinoma (M-85203) Patient id: 614	Lobular carcinoma	negative	https://www.proteinatlas.org/ENSG00000124207-CSE1L/pathology/breast+cancer#img
Female, age 85 Breast (T-04000) Lobular carcinoma (M-85203) Patient id: 614	Lobular carcinoma	negative	https://www.proteinatlas.org/ENSG00000124207-CSE1L/pathology/breast+cancer#img
Female, age 69 Breast (T-04000) Duct carcinoma (M-85003) Patient id: 659	Duct carcinoma	low	https://www.proteinatlas.org/ENSG00000124207-CSE1L/pathology/breast+cancer#img
Female, age 50 Breast (T-04000) Duct carcinoma (M-85003) Patient id: 1271	Duct carcinoma	moderate	https://www.proteinatlas.org/ENSG00000124207-CSE1L/pathology/breast+cancer#img
Female, age 68 Breast (T-04000) Duct carcinoma (M-85003) Patient id: 261	Duct carcinoma	high	https://www.proteinatlas.org/ENSG00000124207-CSE1L/pathology/breast+cancer#img